Fe nanoparticle tailored poly(N-methyl pyrrole) nanowire matrix: a CHEMFET study from the perspective of discrimination among electron donating analytes

2015 J. Phys. D: Appl. Phys. 48 195301

(http://iopscience.iop.org/0022-3727/48/19/195301)

IOP Publishing Journal of Physics D: Applied Physics
J. Phys. D: Appl. Phys. **48** (2015) 195301 (8pp) doi:10.1088/0022-3727/48/19/195301

Fe nanoparticle tailored poly(N-methyl pyrrole) nanowire matrix: a CHEMFET study from the perspective of discrimination among electron donating analytes

K Datta[1,3], P Ghosh[1,3], A Rushi[1], A Mulchandani[2] and M Shirsat[1]

[1] Department of Physics, Intelligent Materials Research Laboratory, Dr. Babasaheb Ambedkar Marathwada University, Aurangabad, Maharashtra, India
[2] Department of Chemical and Environmental Engineering, University of California, Riverside, CA 95616, USA

E-mail: mdshirsat@gmail.com and mds_bamu@yahoo.co.in

Received 16 September 2014, revised 18 January 2015
Accepted for publication 26 February 2015
Published 2 April 2015

Abstract

Back-gated chemically sensitive field effect transistor (CHEMFET) platforms have been developed with electrochemically synthesized poly(N-methyl pyrrole) nanowires by a templateless route. The nanowire matrix has been tailored with Fe nanoparticles to probe their effect in enhancing the sensing capabilities of the nanowire platform, and further to see if the inculcation of Fe nanoparticles is helpful to enhance the screening capability of the sensor among electron donating analytes. A noticeable difference in the sensing behaviour of the CHEMFET sensor was observed when it was exposed to three different analytes—ammonia, phosphine and carbon monoxide. FET transfer characteristics were instrumental in the corroboration of the experimental validations. The observations have been rationalized considering the simultaneous modulation of the work functions of Fe and polymeric material. The real time behaviour of the sensor shows that the sensor platform is readily capable of sensing the validated analytes at a ppb level of concentration with good response and recovery behaviour. The best response could be observed for ammonia with an Fe nanoparticle tailored polymeric matrix, with a sensitivity of ~31.58% and excellent linearity (R^2 = 0.985) in a concentration window of 0.05 ppm to 1 ppm.

Keywords: CHEMFET, poly(N-methyl pyrrole), nanowires, Fe nanoparticles, electron donors

(Some figures may appear in colour only in the online journal)

1. Introduction

Increasing consciousness of efficient monitoring of ambient and workplace air quality has prompted research in a varied class of information acquisition entities called gas sensors. Growing levels of industrialization and urbanization are continuously adding pollutants to the atmosphere, and many of these pollutants can endanger human life even at a sub-ppm level of occurrence in the atmosphere [1]. Alarmingly, such pernicious effects are often too low to be detected at an early stage [2]. Above all, reliable performance of a sensor in ambient atmosphere, a highly complex frame of reference for operation, has always been the prime point of research. The stiff horizon of requisites for a real time sensing device [3], for instance (i) high sensitivity towards trace levels of analytes, (ii) low power consumption, (iii) facile combination with existing electronics, (iv) small physical footprint and (v) fast response and refresh, has geared the spectrum of efforts towards development of tailor-made sensor platforms, and a sound understanding of the underlying sensor mechanism for

[3] These authors contributed equally.

any sensor constitutes the key point to achieve the expected performance level.

The present status of synthesis modalities and operational maneuverability of nanostructured materials suggests that one dimensional (1D) nanostructures are highly potent, with minimal trade-off between cross capabilities in addressing the challenges to emerge as new age sensing materials [4, 5]. Apart from minimization of sensor dimension and requirement for low power electronics to combine with, 1D nanostructures offer a high aspect ratio, that results in charge carrier accumulation or depletion in the bulk of the structure [6], and thus, they are highly sensitive to even minor perturbations in ambient conditions. Among pronounced 1D nanostructures [7–9], conducting polymer (CP) nanowires have succeeded in remaining at the focus of interest for sensor-based applications for decades. This class of materials exhibits unique tunable electronic properties [10–12] that enable acute shaping of band gap structure, which is a prime requisite for gas sensing applications [13]. At the same time, ease of synthesis, and unparallel flexibility and processibility, are advantageous aspects with polymeric materials that are not easy attainable for their counterparts—SWNTs and metal oxide nanowires. In the form of either single nanowires [14, 15] or aligned [16–18]/dendritic nanowire matrix [19] between pre-patterned electrodes, conducting polymer nanowires have shown significant sensing capabilities.

To date, conducting polymers have been extensively used to detect a large variety of analytes/gases; however, the sensing mechanism in most of the observations relies on charge transfer between analytes and the polymeric backbone [14, 15, 17, 20–23]. Selective screening of analytes, thus, remains a high hurdle for polymeric sensors. Several reports have demonstrated modified/functionalized polymers to show enhanced sensing towards particular analytes. Dixit *et al* have found a specific affinity of Fe–Al doped poly(aniline) (PANI) sensors towards CO in contrast to HCN and NH_3 [24]. Paul *et al* have reported that inclusion of ferrocene with poly(pyrrole) resulted in efficient carbon monoxide sensing [25], which was attributed to the transfer of an electron cloud near the carbon atom of CO to the Fe atom of the ferrocenyl moiety. Surprisingly, in striking contrast to the above mechanism, Watcharahalakom *et al* have reported a PANI based CO sensor [26] where they have suggested withdrawing of the electron lone pair from –NH sites of PANI by CO. Such discrepancies in suggested mechanisms definitely warrant systematic studies for effective design of selective sensing backbones based on conducting polymers. Moreover, modification/functionalization of polymers reported to date is more or less based on thin film structures. Recently, Pawar *et al* have demonstrated a PANI–TiO_2 nanofibrous film that shows selective behaviour towards ammonia. The selective nature of the sensor was attributed to creation of a positively charged depletion layer on TiO_2 [27], but the behaviour of the sensor with other analytes was not thoroughly discussed. A significant attempt towards post-synthesis functionalization of polymeric nanowires has been reported by Shirsat *et al* [28], where the authors demonstrated successful ppb level sensing of H_2S with a Au nanoparticle modified PANI nanowire matrix. Liu *et al* have employed a similar sensing backbone to detect volatile sulfur compounds [29]. The significance of this particular approach is manifold—(i) metal nanoparticles enhance the effective surface area, that results in higher surface of interaction with the gas [30], (ii) the catalytic affinity of several metals to particular gas/gases [31], (iii) ease of synthesis of metal nanoparticles on a polymeric surface by the electrochemical route [28], chemical route [29] or thermal/e-beam evaporation [32] and (iv) the chemical library of metals is extensive. However, not much effort has been directed to explore this perspective for development of analyte specific sensors with CPs. Star *et al* have employed this route for development of a gas sensor array by tailoring the surface of chemical vapour deposited SWNTs on an Si platform [32]. To date, most of the investigations on metal nanoparticle decorated SWNT/CP based sensors have relied on noble metals for their catalytic properties [33–35].

In the present investigation, CHEMFETs were fabricated with Fe nanoparticle modified poly(N-methyl pyrrole) (P(NMP)) nanowires, electrochemically synthesized to bridge two Au microelectrodes 3 μm apart on Si substrate, as the active sensing layer. The CHEMFETs were employed to sense ammonia (NH_3), carbon monoxide (CO) and phosphine (PH_3). The choice of metal and analytes was judicial. Instead of looking towards development of a particular sensor, the impetus was to analyze the sensor response towards analytes that are all electron donors. Fe was the particular choice due to its vacant d orbital that is prone to accept electrons [2] for elucidation of the sensing mechanism. The analytes, all having electron donating capability, were therefore of critical interest in view of the metal chosen. P(NMP) was chosen for the nanowire backbone due to the generic high conductivity of the pyrrole group and lower susceptibility to oxygen and humidity [36]. Sensing performances were evaluated in back gated CHEMFET modality. CHEMFET studies, apart from illustrating the sensor performance, were also instrumental in proposing a possible sensing mechanism. The observations, as detailed in the further course of discussion, clearly indicate that the 'charge donation' phenomenon needs to be critically evaluated for designing selective sensing backbones depending on the charge donating capacity of analytes.

2. Experimental details

2.1. Materials

Monomer N-methyl pyrrole (>99%) was procured from ACROS-ORGANICS (Geel, Belgium). Sodium nitrate ($NaNO_3$), ferrous sulfate ($FeSO_4$) and potassium chloride (KCl) (all chemicals were of analytical grade) were purchased from Rankem, India. The monomer was vaccum distilled prior to use and the rest of the chemicals were used as received. HPLC grade water (Rankem) was used for all syntheses and double deionized (DID) water was employed for rinsing purposes unless otherwise specified.

2.2. Sensor substrate

Standard photolithography and lift off techniques were employed to generate specific patterned Au contacts on a heavily doped Si^+ substrate with 300 nm SiO_2 layer. The oxide layer

was deposited by low pressure CVD followed by e-beam and thermal evaporation of 20 nm Cr (adhesion layer) and 180 nm Au layer(s), respectively. The electrode patterns were defined with 3 μm gap between successive electrodes and the widths of the patterns were kept at 200 μm. Substrates were immersed in piranha solution (70% conc. H_2SO_4/30% H_2O_2) followed by rinsing with DID water and dried under N_2 flow before use.

2.3. Fabrication of sensor backbone

The bridging of Au micropatterns by a P(NMP) nanowire network was accomplished electrochemically in a generic three-electrode geometry [37] in a templateless route. The Au pads were wire bonded (West Bond; 7476D) to a custom chip carrier and epoxy glue was stamped onto the bonded regions for reduction of effective surface area to about 37 254 μm^2 (as confirmed under an optical microscope). The working electrode was formed by externally shorting two successive Au electrodes. A Pt wire (CH Instruments, USA; CHI115) and a chlorinated Ag wire (Ag/AgCl wire) served as counter- and reference electrodes respectively. A deoxygenated aqueous solution of N-methyl pyrrole (monomer) and $NaNO_3$ (dopant) served as electrolyte for synthesis of the nanowire matrix. The monomer and dopant were taken in a concentration ratio of 0.5 mM:1.5 mM. A 0.2 μL electrolytic solution was placed onto the Au 'finger-tip' region. The counter- and reference electrodes were precisely poised in contact with the electrolyte via a Probe Station (Ecopia; EPS1000). The typical two-step deposition process consisted of 0.5 mA cm^{-2} anodic current density applied for 20 min followed by 0.02 mA cm^{-2} for 90 min to the working electrodes. The P(NMP) nanowire surface was tailored with Fe nanoparticles under an identical electrochemical set-up, as already described, by cycling potential across the electrodes from +0.2 V to −0.4 V (V/S Ag/AgCl) five times at a scan rate of 20 mV s^{-1}. The electrolyte, in this case, consisted of metal salt $FeSO_4$ (0.5 mM) and supporting electrolyte KCl (1 mM) in aqueous media. A 0.2 μl drop of deaerated electrolyte was dispersed on the synthesized nanowire region before electrodeposition. All electrochemical syntheses were carried out with a CHI 660C electrochemical work station (CH Instruments, USA). After synthesis, the devices were rinsed in DID water to remove excess metal salts and dried under nitrogen flow.

3. Characterization techniques and instrumentation

Morphological studies of the synthesized sensor devices were carried out by scanning electron microscopy (SEM, Jeol JSEM 6360). To ensure the formation of Fe nanoparticle tailored P(NMP) nanowires, the devices were subjected to energy dispersive x-ray spectroscopy (EDAX). Electrical characteristics (*I*/*V* characteristics) of the pristine and surface tailored P(NMP) nanowires were determined by linearly sweeping potential across the devices from −1 V to +1 V and simultaneous recording of the resulting current (linear sweep voltammetry; CHI660C). Transfer characteristics of the devices were studied in back gate modality with a Keithley 2400 source measure unit coupled with an Aplab (India) PPD3003-S programmable power supply with Si as the back gate. The channel current (I_{DS}) was recorded while sweeping the drain–source voltage (V_{DS}) between −15 V and +15 V and keeping the gate potential fixed at −1 V.

For maximum effective exposure of the sensors to analytes, the devices were placed under a small cylindrical quartz flow-through cell (about 8 ml volume) and clamped. Atmospheric isolation was ensured with a sandwiched silicon o-ring between the chip-carrier and cell. Prior to sensing studies, the sensors were exposed to continuous flow of zero air (>98.5%; 200 ml min^{-1}) unless a stable baseline was achieved (typically, about 20 min duration was required for the fabricated devices to reach a steady state). The sensors were tested under various concentrations of NH_3, PH_3 and CO prepared by diluting the analytes in pre-determined volumetric ratio to the carrier (zero air) to obtain the concentrations (at a cumulative flow rate of 200 ml min^{-1}) for which the sensors were validated. The flows of carrier and analyte were regulated by mass flow controllers (Alicat Scientific, MC200). At least eight devices were validated for each analyte to study device to device performance variation.

For CHEMFET modality sensing, transport measurements were made by sweeping the V_{GS} from −15 V to +15 V at a constant V_{DS} of −1 V at 0.25 ppm concentration of analyte in each case. The mode and methods of measurements were the same as applied for studying device transfer characteristics. Real time sensing responses of the devices were studied by applying a constant V_{GS} (optimized from respective transfer characteristics) and recording the I_{DS} under exposure to various concentrations of analytes. During exposure of the analyte at a particular concentration, the sensors were allowed to achieve maximum response immediately followed by flooding with zero air for optimum recovery to complete one validation cycle. Ohm's law was applied to calculate the instantaneous steady state sensor resistance. All syntheses and measurements were carried out under general laboratory conditions unless otherwise specified.

To study the stability of the sensors with reference to time, a typical Fe nanoparticle tailored sensor was tested in 0.5 ppm concentration of ammonia (the particular analyte for which the sensor had shown the best result) at an interval of 5 d and the sensitivity was recorded for a period of 110 d. During the entire experimentation period, the sensor under validation was kept under normal laboratory conditions.

4. Results and discussion

4.1. Electrochemical synthesis

A chronopotentiogram for the synthesis of P(NMP) nanowire devices by a typical two step galvanostatic route [28] is shown in figure 1. In the first step of deposition, a higher current density was applied for formation of polymeric nuclei, that acted as seeds for growth of nanowires in the subsequent phase of deposition. During the first step, the potential across the working electrode (with respect to an Ag/AgCl quasi-reference electrode) was found to be in the range of about 0.62 V. On lowering the current density in the second step, the potential

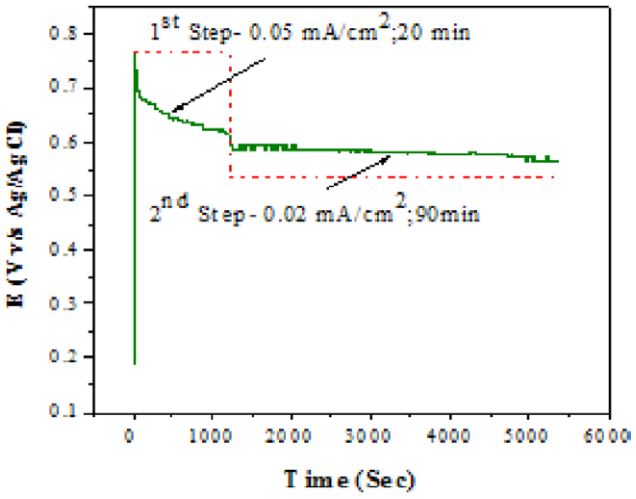

Figure 1. Chronopotentiogram of two step galvanostatic deposition of P(NMP) nanowires.

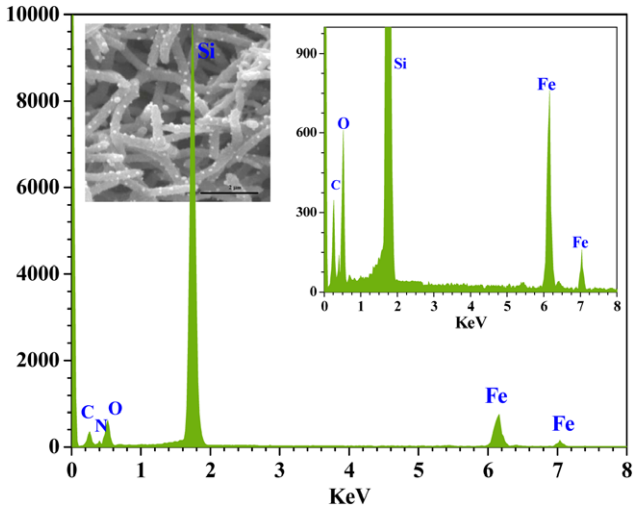

Figure 2. EDAX spectrum of Fe nanoparticle tailored P(NMP) nanowires; (inset) FESEM image of the same.

of the working electrode decreased and gradually stabilized at about 0.57 V, indicating the formation of nanowires [38].

4.2. Elemental analysis and morphological study

As shown in figure 2, different peaks of the EDAX spectrum correspond to the elements C, O, N, Si and Fe for the Fe nanoparticle tailored P(NMP) nanowires and the Si/SiO_2 substrate. The FESEM image (inset to figure 2) of the Fe nanoparticle tailored P(NMP) nanowires shows formation of dendritic nanowires with abundant intertwines. The average diameter of the nanowires was found to lie in the range of 250–350 nm.

The surfaces of synthesized nanowires were found to be smooth and uniform throughout. Similar morphologies of electrochemically synthesized P(NMP) nanowires have been reported by the present author [37]. The distribution of Fe nanoparticles on the surface of the nanowire matrix was found to be uniform, with the average diameter of the nanoparticles lying in the range of 65–80 nm.

4.3. Electrical and FET measurements

The current–voltage (*I*/*V*) characteristics (figure 3) indicate formation of ohmic contacts with Au microelectrodes for both the pristine and surface tailored P(NMP) nanowire networks. As suggested by the transfer characteristics (figure 4), both the devices exhibited p-type nature, confirming that the surface tailoring did not affect the generic nature of the polymeric network. Thus, the ohmic contacts ensured the work function of the P(NMP) nanowire network (both pristine and modified) to be lower than that of Au (ϕ_{Au} = 5.1 eV) [39].

Further, the lower device current observed for the Fe tailored network was indicative of transfer of electrons from Fe nanoparticles to the polymeric backbone decreasing the overall hole concentration. In fact, when a metal and a semiconductor are brought into contact, a charge transfer occurs till their Fermi levels are aligned (under equilibrium conditions). Such a phenomenon is acutely dependent on the work function of the metal and semiconductor and, equally, on the

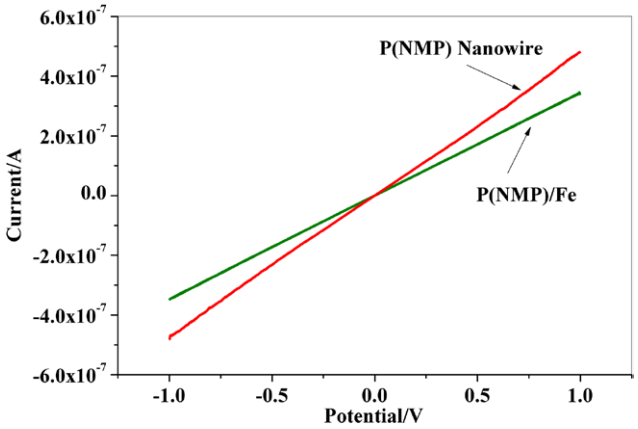

Figure 3. *I*/*V* characteristics of P(NMP) nanowires before and after tailoring of Fe nanoparticles.

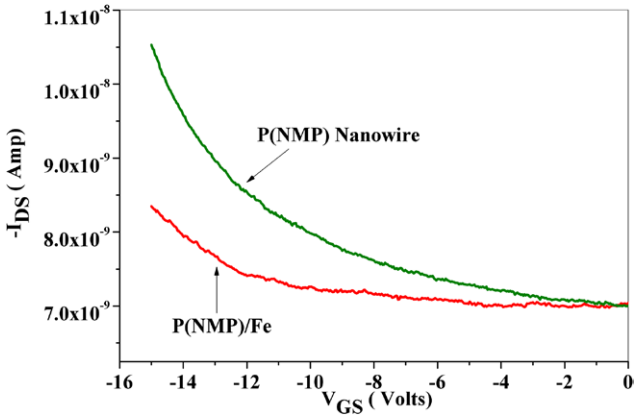

Figure 4. FET transfer characteristics of P(NMP) nanowires before and after tailoring of Fe nanoparticles.

type of semiconductor (p or n), that determines if a Schottky barrier or an ohmic contact will result [40]. As per observations, since the semiconducting backbone was p type in nature and electron donation took place from the metal to the semiconductor, two crucial assumptions could be made. (i) The work function of the P(NMP) nanowire network

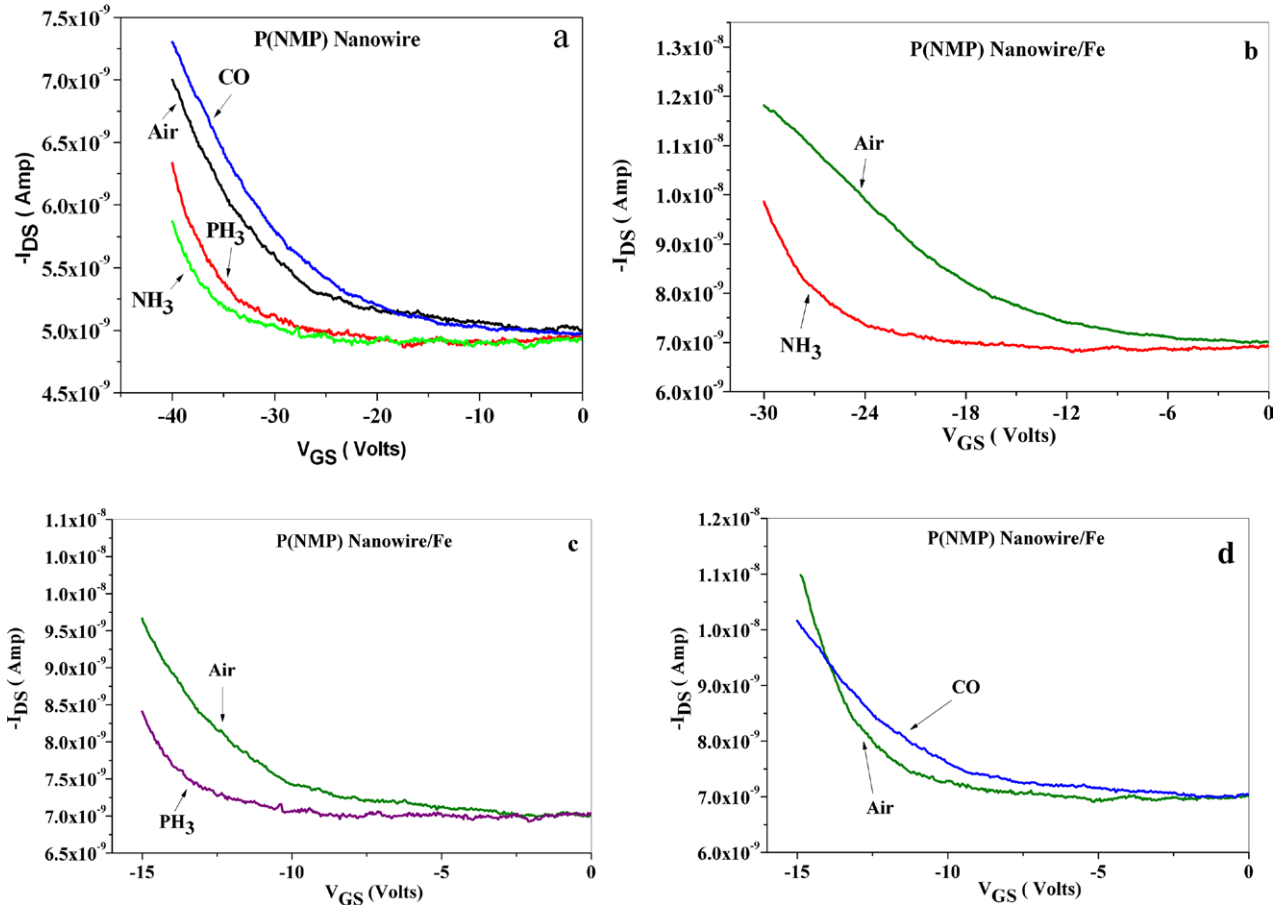

Figure 5. (*a*) FET transfer sensing characteristics of pristine P(NMP) nanowire device for 0.25 ppm concentrations of NH_3, PH_3 and CO; (*b*)–(*d*) FET transfer sensing characteristics of Fe nanoparticle tailored P(NMP) nanowire device for 0.25 ppm concentrations of NH_3, PH_3 and CO respectively.

was greater than that of Fe (ϕ_{Fe} = 4.5 eV). To the best of our knowledge, the work function of P(NMP) is not reported in any literature. However, poly(pyrrole) has been reported to have a work function of 5 eV. (ii) Schottky barriers have been formed at the metal–semiconductor interface. Formation of these Schottky barriers occurs since aligning the Fermi level at equilibrium requires donation of electrons from the metal to the semiconductor (since the work function of P(NMP) is higher than that of Fe), and these electrons are accommodated by a depletion region in which ionized acceptors are left uncompensated by holes [40]. Thus, a potential barrier is formed at the metal nanoparticle–semiconductor interface and the magnitude of the same, as well envisaged, is proportional to the work function difference. The depletion regions, thus formed, act as potential scattering sites [41, 42], that reduces effective carrier mobility and results in overall reduction of device current. This elucidation was further supported by transfer characteristics that show a negative shift of the threshold voltage along with a downward tilt in the transfer curve of the Fe nanoparticle tailored device compared with that of pristine P(NMP) nanowires. As mentioned above, the shift could be well attributed to the donation of electrons from Fe nanoparticles to the P(NMP) nanowires, that reduced the effective hole concentration on the polymeric backbone, whereas the downward tilt was due to the formation of charge depletion sites, that decreases carrier mobility.

4.4. Sensor behaviour

Figure 5(*a*) shows the transfer curves recorded for the pristine nanowire device under ambient atmosphere and 0.25 ppm concentration of all analytes, whereas figures 5(*b*)–(*d*) show transfer curves recorded for Fe nanoparticle tailored P(NMP) nanowire devices for respective analytes at 0.25 ppm concentration.

Under PH_3 and NH_3 atmosphere, the threshold voltage was found to exhibit a negative shift in comparison to the threshold voltage of the device under ambient conditions due to the donation of electrons from analytes to the protonated P(NMP), i.e. $P(NMP)^{H+}$ sites, that reduced effective hole concentration. Since all the analytes under the scanner had lone electron pairs, the 'differences in threshold voltage shifts' needed further consideration. As revealed by the characteristics, the maximum shift in device threshold voltage could be observed under NH_3 atmosphere. A considerably less negative shift could be observed under PH_3 atmosphere. Such behaviour of the sensor for PH_3 indicated a lower tendency of the same to donate electrons than NH_3. Towards finding an explanation for such behaviour of PH_3, the atomic radii of phosphorus (128 pm) and nitrogen (65 pm) were considered. The higher atomic radius of the phosphorus atom results in less electron density on the phosphorus atom in PH_3 than on the nitrogen atom in NH_3. Thus, the inferior sensing behaviour of the sensor towards phosphine

finds a concrete justification. To explain the 'surprising' positive shift observed in CO atmosphere, it was considered that, while on one hand the carbon atom of CO reduces its negative charge by donating its lone pair of electrons, there is an equal possibility of overlapping of unfilled d orbitals of the carbon atom with the delocalized π orbital of the P(NMP) backbone, accepting electrons. In fact, under such situations, CO can act as both electron donor and acceptor [31]. The behaviour of the sensor under CO atmosphere was definitely shaped by these opposite charge transfer phenomena and the electron acceptor nature of CO played a dominant role. Equally, the observed positive shift was found to be less than the negative shift observed for NH_3. Thus, the electron donating capability of the analytes might be considered to play a major factor to decide sensor behaviour [43]. Further, the absence of any characteristic tilt in transfer curves allowed us to infer that the analyte induced modulations in work functions of either P(NMP) or Au, in the contact region, had not significantly modulated the contact properties. Basically, formation of ohmic contacts, as described earlier, offers a very small barrier for flow of charge carriers at the metal–semiconductor junction region [40], and from observations it was ensured that, under the exposure of analytes, contact properties were not varied significantly.

The Fe nanoparticle tailored devices exhibited significantly distinguishable 'shift' and additionally 'tilt' in respective analyte atmospheres. Such observations are clear denotations of the effect of Fe nanoparticles on modulating the sensing behaviour and enhancing the screening capability of the sensor backbone. The vacant d orbitals in Fe acted as potential electron accepting sites [2], and as per the electron donating capability of the analytes, as already discussed, the 'shifts' in device threshold voltages (due to lowering of 'holes', an immediate effect of recombination) were shaped. As evident from figures 5(*b*)–(*d*), the 'shifts' were more significant than in pristine P(NMP) devices. To elucidate the observed 'tilts' in the transfer curves, (i) concurrent modulation in work functions of P(NMP) [44] and Fe [45] due to electron donation from the analytes and (ii) the recombination phenomenon at the nanoparticle/nanowire interface sites [41] were considered. The observations could find a plausible rationalization in that the modulation of work function(s) resulted in shaping the contact potential barriers in accordance with the electron donating tendencies of the analytes. In this domain, electron donation from NH_3 and PH_3 might result in more profound lowering of the work function of the P(NMP) backbone at nano-Schottky [46] barriers than that of Fe nanoparticles, lowering the overall contact potential. However, in such a situation, a downward tilt in the device transfer characteristic was expected due to recombination at the interface sites. The upward tilt, however, suggested that the P(NMP) Fermi level was raised more significantly than that of Fe, which effectively reduced the contact potential difference between them. As a result, the impact of the depletion layer created due to recombination at the interfacial sites was less significant than it was in air; hence, the effective charge carrier mobility increased and an upward tilt was recorded in the device transfer characteristic under exposure to NH_3. Due to the lower electron donating capacity of PH_3, the upward tilt was observed to be less significant, for the reason already proposed. The behaviour of the sensor for CO was again a cumulative effect of electron donation from CO to Fe and from P(NMP) to CO, as already discussed. The downward tilt might be indicative of the fact that electron donation from P(NMP) to CO was a more dominant phenomenon that resulted in lowering of the Fermi level, whereas, even if lower, donation of electrons from CO to Fe ought to raise the Fermi level in Fe. These simultaneous phenomena resulted in enhancing the contact potential difference between Fe and P(NMP) at the interfacial sites (it may be noted that this is the completely opposite phenomenon to the cases of NH_3 and PH_3), resulting in a significant role of the depletion layer at the interfacial sites in decreasing overall charge carrier mobility. A downward tilt was consequently observed in the device transfer characteristic recorded in CO atmosphere.

Figure 6(*a*) shows real time sensing behaviour (in terms of normalized changes in resistance ($\Delta R/R_0 = (R - R_0)/R_0$; where R_0 = baseline resistance of the sensor and R = steady resistance of the sensor at certain concentration of analyte) of the Fe nanoparticle tailored P(NMP) nanowire matrix for a 0.05 ppm to 1 ppm concentration window of each analyte. Well defined sensing behaviour in each case could be characterized by sharp response and clear recovery behaviour. For NH_3 and PH_3, device resistance was found to increase with introduction of analytes and decrease upon flushing with zero air. However, for CO, the opposite phenomenon could be observed with markedly weak sensor response. For ammonia (and even phosphine), the sensor exhibited quick response and recovery. For CO, a sluggish behaviour was exhibited, that was perhaps due to the opposite electron transfer behaviour as discussed above. At higher levels of concentration of the analytes (beyond 100 ppm concentration for CO, 135 ppm for PH_3, and 155 ppm for NH_3; data not shown), partial and slow recovery could be observed, that indicated adsorption of analytes at the cross-over sites of the nanowires. Figures 6(*b*) and (*c*) give the calibration for the Fe nanoparticle tailored devices for the respective analytes for lower (0.05–1 ppm) and higher (5–40 ppm) concentration windows of validation, whereas figure 6(*d*) represents the calibration for pristine nanowire based devices in the concentration window of 5–40 ppm. The pristine P(NMP) nanowire sensor response was not reliable in the concentration range of 0.05–1 ppm, as the signal to noise ratio failed to register at the standard set by IUPAC [47]. Hence, it was concluded that the pure P(NMP) based sensors were not capable of sensing the analytes reliably for analyte concentrations of 1 ppm or less and the results were reflected only for the higher range of concentration (5–40 ppm) for validation. The sensitivity and linearity behaviour, as reflected from the trendline equations and the R^2 values, clearly indicates that the best sensing behaviour could be recorded for ammonia, while for carbon monoxide the sensing behaviour was most inefficient. Thus, the recombination phenomenon at interface sites was found to give a less effective sensing mechanism in deciding overall device characteristic. Device to device variation, overall, was found to be trivial. The best sensing platform (i.e. Fe nanoparticle tailored P(NMP) nanowire based devices) showed a sensitivity of 31.58% with excellent linearity ($R^2 = 0.985$ as given

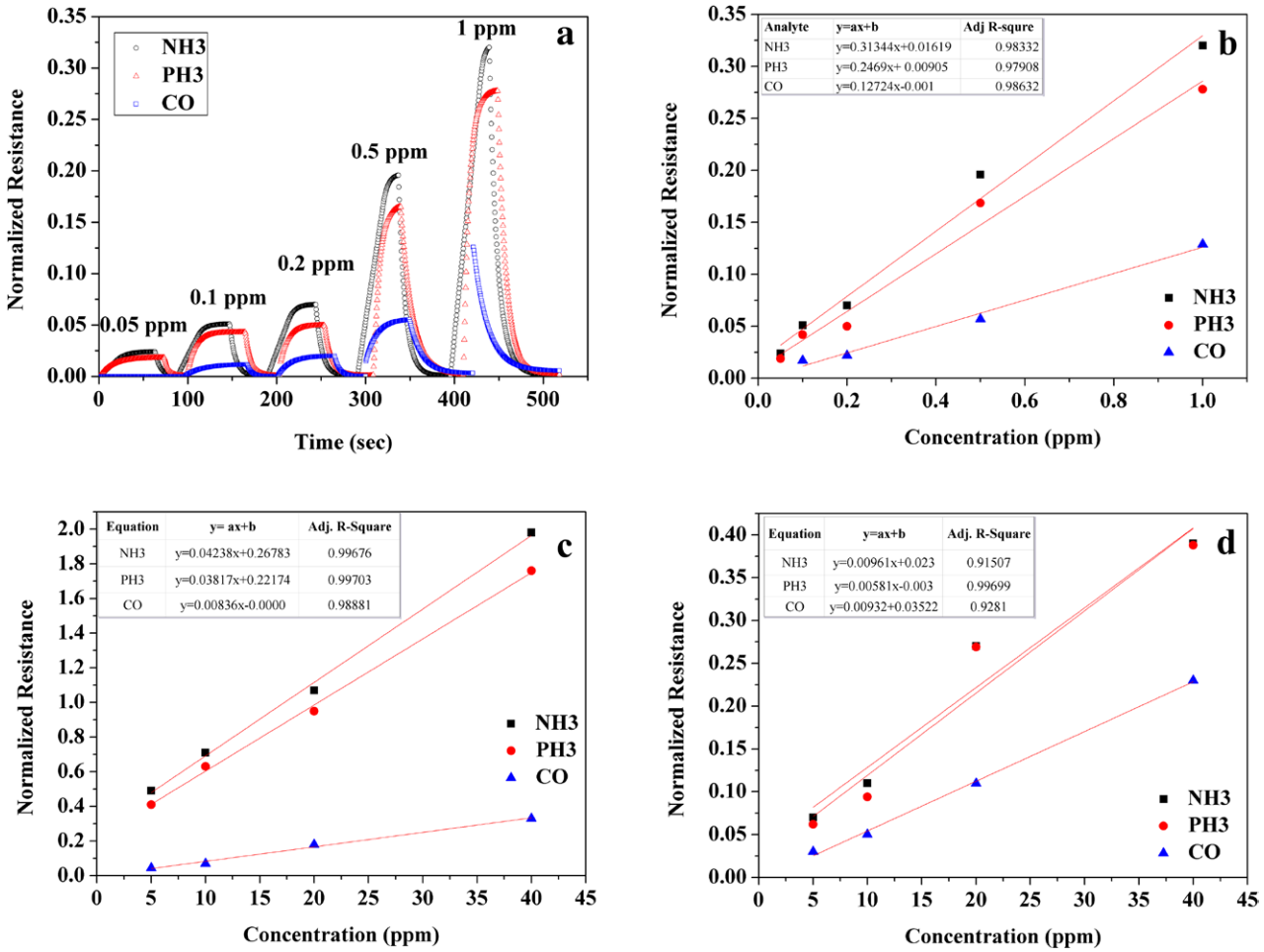

Figure 6. (*a*) Real-time behaviour of Fe nanoparticle decorated P(NMP) nanowires for 0.05–1 ppm concentration of NH_3, PH_3 and CO respectively; (*b*), (*c*) calibration plots for Fe nanoparticle decorated P(NMP) nanowires for (*b*) 0.05–1 ppm and (*c*) 5–40 ppm concentration windows of each analyte; (*d*) calibration plots for pristine P(NMP) nanowires for 5–40 ppm concentration window of each analyte. Results of at least eight validated devices have been represented in each case. It should be noted that only absolute values for normalized resistance (ΔR/RO) has been considered, hence, for CO, the plots are presented in X-axis.

by linear curve fit) for an ammonia concentration window of 0.05–1 ppm.

4.5. Stability characteristic

Figure 7 gives the stability characteristic of Fe(PNMP) sensors in terms of their sensitivity recorded under exposure to 0.5 ppm concentration of ammonia every 5 d. The experiment was carried out for 110 d and the sensor showed reliable sensing till the 83rd day, during which the sensitivity deviated by a factor of 14.22% of from its initial value. Afterwards, the sensor performance deteriorated drastically, maybe owing to natural degradation of the polymer.

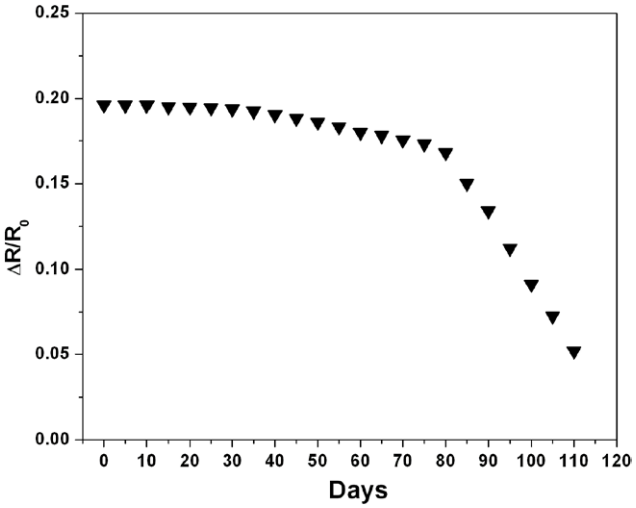

Figure 7. Stability curve for Fe nanoparticle decorated P(NMP) nanowires at 0.5 ppm concentration of ammonia.

5. Conclusions

The electrochemical route proved to be a facile technique for surface tailoring of Fe nanoparticles on P(NMP) nanowire matrices. Due to the relative positions of the Fermi levels in Fe and P(NMP), Schottky barriers were found to form at the nanoparticle/nanowire interface sites, that had an adverse effect on device carrier mobility. However, enhanced sensing behaviour could be achieved after Fe nanoparticle tailoring of the nanowire surface. On exposure to three different entities (ammonia, phosphine and carbon monoxide) with equivalent

electron donating characteristics, the behaviours of the sensors were found to be pivotally dependent on the recombination characteristics at nanoparticle/nanowire interface sites and equally on the modulation of the work function in the semiconductor and the metal. The sensing mechanism was critically decided by a combinational effect with work function modulation having the more dominant role. The inferior performance of the sensor for CO was attributed to the simultaneous electron accepting nature of the analyte. Through the present study, we have been able to differentiate among NH_3, PH_3 and CO in terms of sensitivity. Designing simple comparator and logic based hardware, afterwards, might definitely guide us towards a sensing device with absolute selectivity among the three analytes we have investigated.

The observations suggest that a sensitive look at the work functions of the tailoring metal and the host semiconductor is required to preferably ensure a Schottky barrier formation at the interface; this is instrumental in shaping significant sensor response and screening among electron donating analytes. However, formation of an ohmic contact might also be valuable if the modulation in the cumulative differential work function of the metal and the semiconductor is significantly deviated by the analyte towards formation of a Schottky barrier. This is definitely a significant step keeping in view the plethora of polymeric sensors developed to date whose mechanisms have been defined in terms of charge transfer.

Acknowledgment

The authors (KD, PG, AR, MDS) express their sincere thanks to the Department of Science and Technology (DST)—TSD, New Delhi, India (grant no DST/TSG/PT/2010/11-C & G), and Nanomission, Department of Science and Technology (India), for financial assistance under project no SR/NM/NS-94/2009 dated 9 September 2010.

References

[1] Cheremisinoff N P 2000 *Handbook of Hazardous Chemical Properties* (Boston: Butterworth-Heinemann)
[2] Rushi A, Datta K, Ghosh P, Mulchandani A and Shirsat M D 2013 *Mater. Lett.* **96** 38
[3] Li J, Lu Y, Ye Q, Delzeit L and Meyappan M 2005 *Electrochem. Solid State Lett.* **8** H100
[4] He H and Tao N J 2003 *Encyclopedia of Nanoscience and Nanotechnology* vol X, ed H S Nalwa (New York: American Scientific) p 1
[5] Ding B, Wang M, Yu J and San G 2009 *Sensors* **9** 1609
[6] Wanekaya K, Chen W, Myung N V and Mulchandani A 2006 *Electroanalysis* **18** 533
[7] Kauffman R and Star A 2008 *Angew. Chem., Int. Edn* **47** 6550
[8] Chen P, Shen G and Zhou C 2008 *IEEE Trans. Nanotechnol.* **7** 668
[9] Bangar M A, Chen W, Myung N V and Mulchandani A 2010 *Thin Solid Films* **519** 964
[10] MacDiarmid G 2002 *Synth. Met.* **125** 11
[11] Shirakawa H 2002 *Synth. Met.* **125** 3
[12] Heeger J 2002 *Synth. Met.* **125** 23
[13] Janata J and Josowicz M 2003 *Nat. Mater.* **2** 19
[14] Hernandez S C, Chaudhuri D, Chen W, Myung N V and Mulchandani A 2007 *Electroanal.* **19** 2125
[15] Kim D and Yoo B 2011 *Sensor Actuators* B **160** 1168
[16] Wang J, Chan S, Carlson R R, Luo Y, Ge G, Ries R S, Heath J R and Tseng H R 2004 *Nano Lett.* **4** 1693
[17] Yan X B, Han Z J, Yang Y and Tay B K 2007 *Sensor Actuators* B **123** 107
[18] Dan Y, Cao Y, Mallouk T E, Johnson A T and Evoy S 2007 *Sensors Actuators* B **125** 55
[19] Dong B, Lu N, Zelsmann M, Kehagias N, Fuches H, Torrers C M S and Chi L 2006 *Adv. Funct. Mater.* **16** 1937
[20] Liu H, Kaneoka J, Czaplewski D and Craighead H 2004 *Nano Lett.* **4** 671
[21] Karat H J, Kakde K P, Savale P A, Datta K, Ghosh P and Shirsat M D 2007 *Polymer. Adv. Technol.* **18** 397
[22] Sengupta P P, Barik S and Adhikari B 2006 *Mater. Manuf. Process.* **21** 263
[23] Kukla L, Shirshov Yu M and Piletsky S A 1996 *Sensors Actuators* B **37** 135
[24] Dixit V, Misra S C K and Sharma B S 2005 *Sensors Actuators* B **104** 90
[25] Paul S, Chavan N N and Radhakrishanan S 2009 *Synth. Met.* **159** 415
[26] Watcharaphalakom S, Rauangchuay L, Chotapattanont D, Sirivat A and Schwank J 2005 *Polym Int*. **54** 1126
[27] Pawar S G, Chougule M A, Sen S and Patil V B 2012 *J. Appl. Polym. Sci.* **125** 1418
[28] Shirsat M D, Bangar M A, Deshusses M A, Myung N V and Mulchandani A 2009 *Appl. Phys. Lett.* **94** 083502
[29] Liu C, Hayashi K and Toko K 2012 *Sensor Actuators* B **161** 504
[30] Umar A and Hahn Y B (ed) 2010 *Metal Oxide Nanostructures and Their Applications* vol **3**, ch 2 (Stevenson Ranch, CA: American Scientific) pp 31–52
[31] Shriver D F and Atkins P W 1999 *Inorganic Chemistry* vol **1**, 3rd edn (Oxford: Oxford University Press) ch 17, pp 604–6
[32] Star A, Joshi V, Skarupo S, Thomas D and Gabriel J C P 2006 *J. Phys. Chem.* B **110** 21014
[33] Mubeen S, Zhang T, Charoluprayoon N, Rheem Y, Mulehandani A, Myung N V and Desshuesses M A 2010 *Anal. Chem.* **82** 250
[34] Zanolli Z, Leghrib R, Felten A, PireauX J J, Llobet E and Charlier J C 2011 *ACS Nano* **5** 4592
[35] Penza M, Rossi R, Alvsi M and Serra E 2010 *Nanotechnology* **21** 105501
[36] Kanzawa K K, Diaz A F, Korunbi M T and Street G B 1981 *Synth. Met.* **4** 119
[37] Datta K, Ghosh P, More M A, Shirsat M D and Mulchandani A 2012 *J. Phys.* D*: Appl. Phys*. **45** 355305
[38] Liang L, Liu J, Windisch C F Jr, Exarchos G J and Lin Y 2002 *Angew. Chem. Int. Edn* **41** 3665
[39] Abthagir P S and Saraswathi R J 2001 *J. Appl. Polym. Sci*. **81** 2127
[40] Streetman B G and Banerjee S 2000 *Solid State Electronic Devices* vol **1**, 5th edn (Singapore: Pearson Education) ch 5, pp 220–6
[41] Kauffman R and Star A 2007 *Nano Lett.* **7** 1863
[42] Mubeen S, Lim J H, Srirangarajan A, Mulchandani A, Desshusses M A and Myung N V 2011 *Electroanalysis* **23** 2687
[43] Xing W, Hu J, Kung S C, Donavan K C, Yan W, Wu R and Penner R M 2012 *Nano Lett.* **12** 1729
[44] Chattopadhyay D and Rakshit P C 2009 *Quantum Mechanism, Statistical Mechanics and Solid State Physics* 5th rev. edn (Delhi: Chand) p 231
[45] Pillai S O 2005 *Solid State Physics* vol **1**, 6th edn (New Delhi: New Age International) ch 6, pp 220–3
[46] Ruffino F, Grimaldi M G, Giannazo F, Roccaforte F and Raineri V 2006 *Appl. Phys. Lett.* **89** 243113
[47] Currie L A 1995 *Pure Appl. Chem.* **67** 1699–723